

# Electron impact dissociative ionization of carbonyl chlorofluoride

Pengqian Wang\*, C.R. Vidal

*Max-Planck-Institut für extraterrestrische Physik, Postfach 1312, 85741 Garching, Germany*

Received 23 February 2004; accepted 6 April 2004

Available online 19 June 2004

## Abstract

Electron impact dissociative ionization of carbonyl chlorofluoride (COFCl) has been studied at an electron energy of 200 eV. The dissociation channels of up to triply ionized COFCl are investigated by two- and three-dimensional covariance mapping techniques. The absolute cross sections for the different dissociation channels are measured. The major ionic fragments from the dissociation of COFCl<sup>+</sup> are COF<sup>+</sup> and Cl<sup>+</sup>. The COFCl dications dissociate mainly into ion pairs, among which the first few abundant channels are CO<sup>+</sup> + Cl<sup>+</sup>, C<sup>+</sup> + O<sup>+</sup> and Cl<sup>+</sup> + COF<sup>+</sup>. The COFCl trications dissociate mainly into ion triples, where each dissociation channel has a comparable cross section. © 2004 Elsevier B.V. All rights reserved.

*Keywords:* Electron impact ionization; Multiply ionized molecule; Fragmentation pathway; Covariance mapping; COFCl

## 1. Introduction

The extensive study of electron impact dissociative ionization in recent years is motivated by its increasing use in our modern science and technology. For example, electron collisions in feed gases are the driving mechanisms for plasma processing in semiconductor manufacturing [1,2]. In astrophysics, electron impact ionization is important for the understanding of the products from the ion-molecular reactions in interstellar environment [3]. In both cases cross section data for electron impact ionization are currently urgently needed. However, all the measured cross sections up to now are mostly limited to the total cross section, which corresponds to the production of all the ions, or the partial cross section, which corresponds to the production of a specific ion. If we keep in mind that upon electron impact the molecules can be ionized to different stages, i.e., single, double, and higher ionization stages, we are naturally confronted with one interesting question: how much does each ionization stage contribute to a specific ion product? To answer this question the various dissociation channels must be distinguished by a coincidence technique and measured separately. On the other hand, the dissociation dynamics re-

trieved from the coincidence detection can provide valuable information on the electronic states and potential energy surfaces of multiply ionized molecules, and greatly increase our knowledge on the structure of molecular ions [4,5].

Carbonyl chlorofluoride (COFCl) is an interesting molecule of atmospheric importance. It is among the first stable decomposition products of various chlorofluorocarbons and hydro-chlorofluorocarbons [6,7], and has been observed in the stratosphere [8]. The structure of COFCl has been explored by studying its electronic, vibrational, and rotational spectra [9–13], and by studying its dissociation mechanisms in photolysis [7,8,14–16]. However, there was no attempt in probing COFCl in its ionic states. In this paper we investigate the dissociation of singly to triply ionized COFCl produced by electron impact ionization. The dissociation channels are distinguished by two- and three-dimensional covariance mapping techniques, and the cross section for each dissociation channel is measured. The electron beam energy was set to 200 eV. This energy has been used because firstly we expect that like in the case of other molecules, such as CO [17], CO<sub>2</sub> [18], N<sub>2</sub>, and O<sub>2</sub> [19], at this energy the cross sections for most of the dissociation channels are close to their maxima and thus can be easily measured. Secondly, above 200 eV the relative cross sections for most of the dissociation channels do not change too much [17–19], which makes this energy representative for probing the fragmentation patterns in electron impact ionization.

\* Corresponding author. Present address: J.R. Macdonald Laboratory, Department of Physics, Kansas State University, Manhattan, KS 66506, USA. Tel.: +1 785 532 2669; fax: +1 785 532 6806.

*E-mail address:* [pqwang@phys.ksu.edu](mailto:pqwang@phys.ksu.edu) (P. Wang).

## 2. Experimental setup and data-processing method

The experimental setup for electron impact ionization has been described in detail elsewhere [18], therefore only a brief description is given here. The molecular beam of interest is emitted continuously from a long needle, which is then skimmed and crossed by a pulsed electron beam. A focusing time-of-flight mass spectrometer [20], which is modified from a normal Wiley-McLaren mass spectrometer, is used to collect the ionic fragments. The ions are detected by a microchannel plate and recorded by a multichannel scaler. Using proper voltage settings for the focusing time-of-flight mass spectrometer, the ions with initial kinetic energies up to 25 eV/charge can be collected with the same efficiency as that of the thermal ions. The experiment is performed with totally  $7 \times 10^8$  electron pulses. The repetition rate of the electron pulse is 4 kHz, and the counting rate of the ion fragments is controlled to be 0.7 ion/pulse. The COFCl gas is purchased from ABCR GmbH with a purity of 97%, and is used without further purification. The ion count from the background gases, which is less than 5% of COFCl, is subtracted from the mass spectrum and the covariance map.

The covariance mapping technique was first introduced to the dissociation of molecular ions by Frasiniski et al. [21]. The principle is briefly as follows. Let  $X_n(i)$  be the single pulse TOF spectrum for the  $n$ th pulse, where  $i$  is the time-bin of the multichannel scaler. The second order covariance function of  $X_n(i)$  is:

$$\begin{aligned} C_2(i, j) &= N \overline{(X_n(i) - \overline{X_n(i)})(X_n(j) - \overline{X_n(j)})} \\ &= \sum_{n=1}^N X_n(i)X_n(j) - \frac{1}{N} \sum_{n=1}^N X_n(i) \sum_{n=1}^N X_n(j). \end{aligned} \quad (1)$$

Here  $N$  is the total number of pulses. The averages are taken over all the pulses. The first term of Eq. (1) is the total double coincidence, and the second term represents the false coincidence, where the two ions come from different parent ions. If we plot  $C_2(i, j)$  on a plane we get a *covariance map*. Similarly the third order covariance function of  $X_n(i)$  is:

$$\begin{aligned} C_3(i, j, k) &= N \overline{(X_n(i) - \overline{X_n(i)})(X_n(j) - \overline{X_n(j)})(X_n(k) - \overline{X_n(k)})} \\ &= \sum_{n=1}^N X_n(i)X_n(j)X_n(k) - \frac{1}{N^2} \sum_{n=1}^N X_n(i) \sum_{n=1}^N X_n(j) \\ &\quad \times \sum_{n=1}^N X_n(k) - \frac{1}{N} \sum_{n=1}^N (C_2(i, j)X_n(k) \\ &\quad + C_2(i, k)X_n(j) + C_2(j, k)X_n(i)). \end{aligned} \quad (2)$$

Here the first term is the total triple coincidence, and the other terms represent the false coincidence, where the ions either come from three different parent ions or two of them come from one parent ion and the third one comes from another. If we plot  $C_3(i, j, k)$  in the space we get a three-dimensional covariance map, or a *covariance volume*.

Table 1

The dissociation channels for up to triply ionized COFCl

Parent ion	Dissociation channel	Cross section
COFCl <sup>+</sup>	→ X <sup>+</sup> + n	$\sigma_1(X^+)$
COFCl <sup>2+</sup>	→ X <sup>2+</sup> + n	$\sigma_2(X^{2+})$
	→ X <sup>+</sup> + Y <sup>+</sup> + n	$\sigma_2(X^+, Y^+)$
COFCl <sup>3+</sup>	→ X <sup>2+</sup> + Y <sup>+</sup> + n	$\sigma_3(X^{2+}, Y^+)$
	→ X <sup>+</sup> + Y <sup>+</sup> + Z <sup>+</sup> + n	$\sigma_3(X^+, Y^+, Z^+)$

The symbol “n” denotes the neutral fragments if they exist.

Since upon electron impact the molecules are mainly ionized into lower stages, the ionization orders considered in our work are limited to single to triple ionization. Higher order ionizations exist in much smaller quantities and they demand much longer data acquisitions. All the possible dissociation channels after single, double, and triple ionization are divided into five groups as listed in Table 1. No trication is observed in the mass spectrum, so the corresponding channels are omitted in the table. The neutral fragments are not recorded in our experiment. For the sake of brevity we use the symbol “n” to represent all the neutral fragments if they exist. The cross section for each channel is denoted in the last column.

In order to measure the absolute partial cross section of an ion, we use argon as a reference gas. In the course of calibration argon and COFCl are mixed in the reservoir at equal partial pressures. The gas flow in the experiment is kept in the effusive flow regime. The partial cross section of a specific ion X<sup>+</sup> (and similarly X<sup>2+</sup>) is given by:  $\sigma(X^+) = n_1(X^+)\sigma(\text{Ar}^+)/n_1(\text{Ar}^+)$ , where  $n_1(X^+)$  is the ion count of X<sup>+</sup> in the mass spectrum. The cross section of Ar<sup>+</sup> has been well established, and we use the data of Straub et al. [22], which is  $2.18 \times 10^{-16} \text{ cm}^2$ , as a reference.

The absolute cross sections for the dissociation channels that produce an ion pair or an ion triple can be calculated by:

$$\begin{aligned} \sigma_2(X^+, Y^+) &= \left( \frac{n_2(X^+, Y^+)}{T\eta} - \sum_{Z^+} \frac{n_3(X^+, Y^+, Z^+)}{(T\eta)^2} \right) \frac{\sigma_{\text{total}}}{n_{\text{total}}}, \end{aligned} \quad (3)$$

$$\sigma_3(X^{2+}, Y^+) = \frac{n_2(X^{2+}, Y^+)}{T\eta} \frac{\sigma_{\text{total}}}{n_{\text{total}}}, \quad (4)$$

$$\sigma_3(X^+, Y^+, Z^+) = \frac{n_3(X^+, Y^+, Z^+)}{(T\eta)^2} \frac{\sigma_{\text{total}}}{n_{\text{total}}}. \quad (5)$$

Here  $n_2$  is the ion-pair count inside an area on the covariance map, and  $n_3$  is the ion-triple count inside a block in the covariance volume. Since  $n_3(X^+, Y^+, Z^+)$  intrinsically contributes to  $n_2(X^+, Y^+)$ , it is subtracted when calculating  $\sigma_2(X^+, Y^+)$ . The value of  $\sigma_{\text{total}}$  is the total cross section of the ions, and  $n_{\text{total}}$  is the total ion count.  $T$  is the total transmission of the meshes in the mass spectrometer, and  $\eta$  is the detection efficiency of the microchannel plate.  $T$  is taken from the open area ratio in the manufacturer's manual, which is 58.1% and agrees with the optical transparency

of the meshes. For  $\eta$  we use the open area ratio from the manufacturer's manual, which is 54.5%. It has been shown experimentally that the detection efficiency of the microchannel plate is equal to its physical open area ratio [22–24]. The remaining cross sections, i.e.,  $\sigma_1(X^+)$  and  $\sigma_2(X^{2+})$ , can be easily derived from the following sum rules:

$$\sigma(X^+) = \sigma_1(X^+) + \sum_{Y^+} \sigma_2(X^+, Y^+) + \sum_{Y^{2+}} \sigma_3(Y^{2+}, X^+) + \sum_{Y^+, Z^+} \sigma_3(X^+, Y^+, Z^+), \quad (6)$$

$$\sigma(X^{2+}) = \sigma_2(X^{2+}) + \sum_{Y^+} \sigma_3(X^{2+}, Y^+). \quad (7)$$

The errors in the absolute cross sections have been estimated elsewhere [18]. It is mainly caused by the error in the normalization of the cross sections, the error in the transmission of the meshes and that in the detection efficiency of the microchannel plate. The error in the partial cross section of an ion is estimated to be 10%, and that for an ion pair is about 20%. For the ion triples, and for the dissociation channels that produce only one ionic fragment, the errors are expected to be about 25%.

### 3. Results and discussion

#### 3.1. Covariance map

The electron impact mass spectrum of COFCl at 200 eV is shown in Fig. 1. Some dications have been amplified to show the details. The main part of the covariance map, which contains all the major dissociation channels of COFCl<sup>2+</sup>, is shown in Fig. 2. The positions of the mass peaks observed in Fig. 1 are displayed in the bottom and on the left.

On the covariance map, the area that contains the ion-pair count for a certain dissociation channel is called an *island*. Some of the islands in Fig. 2 are enlarged and displayed in Fig. 3a–d, they correspond to Cl<sup>+</sup> + COF<sup>+</sup>, CO<sup>+</sup> + Cl<sup>+</sup> + F, CF<sup>+</sup> + Cl<sup>+</sup> + O, and C<sup>+</sup> + Cl<sup>+</sup> + n, respectively. All the islands in Fig. 3 have well-defined shapes and orientations. The orientation angle of an island, defined as the angle

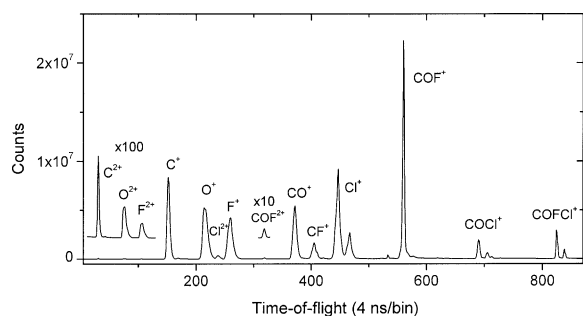


Fig. 1. The time-of-flight mass spectrum of COFCl. The electron energy is 200 eV.

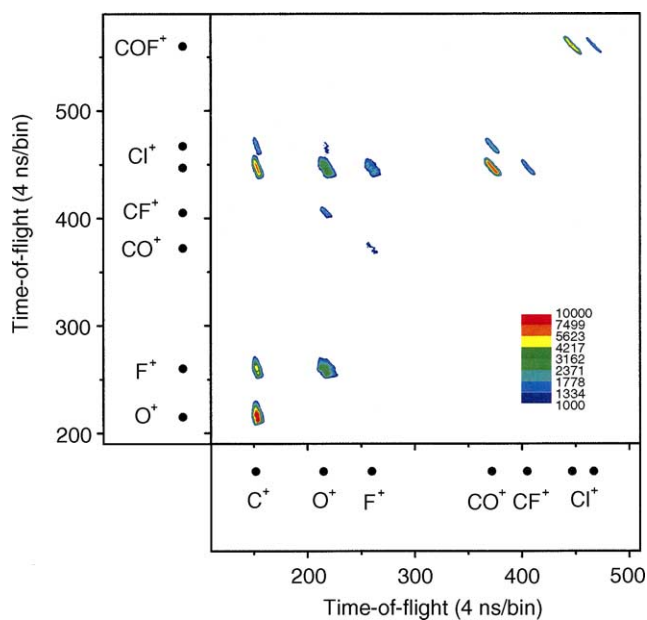


Fig. 2. Part of the covariance map for electron impact ionization of COFCl. The positions of the mass peaks are shown in the bottom and on the left.

between the major axis of the island and the  $x$ -axis of the map, can be calculated by  $\arctan(p_y q_x / p_x q_y)$ , where  $q$  and  $p$  are the charge and momentum of the fragment ions [25]. The geometrical characters of an island, especially its orientation angle, are important in retrieving the dissociation dynamics and kinetics [18,25–28]. For a two-body separation, such as Cl<sup>+</sup> + COF<sup>+</sup> in Fig. 3a, since the two fragments carry equal momentum and fly in opposite directions, the island should orient at  $-45^\circ$ . The measured angle for Cl<sup>+</sup> + COF<sup>+</sup> is  $-45.1 \pm 0.8^\circ$ , which agrees well with this prediction.

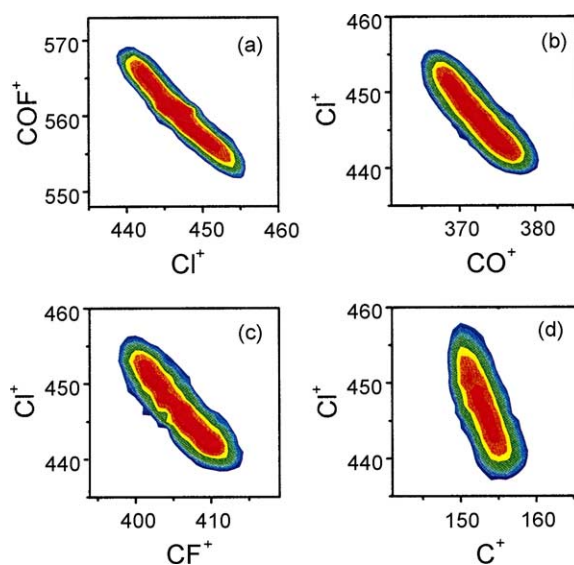


Fig. 3. The islands for some of the ion-pair dissociation channels of COFCl<sup>2+</sup>. (a) Cl<sup>+</sup> + COF<sup>+</sup>, (b) CO<sup>+</sup> + Cl<sup>+</sup> + F, (c) CF<sup>+</sup> + Cl<sup>+</sup> + O and (d) C<sup>+</sup> + Cl<sup>+</sup> + n. The contours are in logarithmic scale and increase five times from the side to the center.

For a three-body separation, sequential dissociation through initial charge separation is often utilized to interpret the observed characters of an island [18,26]. For Fig. 3b, the supposed process is (1)  $\text{COFCI}^{2+} \rightarrow \text{COF}^+ + \text{Cl}^+$  and then (2)  $\text{COF}^+ \rightarrow \text{CO}^+ + \text{F}$ . The kinetic energy release in the second step is much smaller than in the first step. If the second step happens beyond the Coulomb effective area of  $\text{Cl}^+$ , the island should orient at  $\arctg(\text{COF}/\text{CO}) = -59.2^\circ$ . If the second step occurs very close to  $\text{Cl}^+$ , the process will converge into a simultaneous explosion, and the orientation of the island should be near  $-45^\circ$ . The measured orientation angle of this island is  $-48.8 \pm 1.2^\circ$ , which is larger than  $-45^\circ$  but smaller than the out-of-Coulomb field limit as mentioned above. This implies that  $\text{COF}^+$  breaks up at a short distance to  $\text{Cl}^+$ . Similarly, Fig. 3c can be explained as (1)  $\text{COFCI}^{2+} \rightarrow \text{COF}^+ + \text{Cl}^+$  and then (2)  $\text{COF}^+ \rightarrow \text{CF}^+ + \text{O}$ . Here the orientation angle for the out-of-Coulomb field limit is  $\arctg(\text{COF}/\text{CF}) = -56.6^\circ$ , while the measured angle is  $-49.5 \pm 1.2^\circ$ , again suggesting that  $\text{COF}^+$  dissociates inside the Coulomb field of  $\text{Cl}^+$ . Fig. 3d is a four-body separation, the explanation is complicated. However, it can be seen that  $\text{C}^+$  carries a small but nearly fixed portion of momentum compared to that of  $\text{Cl}^+$ .

The covariance volume cannot be directly drawn on paper. Inside the covariance volume, the region that contains the ion-triple count for a certain dissociation channel is called a *cell*. In Fig. 4 we show the projections of one of the cells,  $\text{COFCI}^{3+} \rightarrow \text{C}^+ + \text{F}^+ + \text{Cl}^+ + \text{O}$ , on three mutually perpendicular planes. The actual shape of this cell can be imagined if we fold up the  $x-z$  and  $y-z$  planes along the dashed borders. All three islands have negative orientation angles, this means that the angles between each two momenta are larger than  $90^\circ$ . The islands on the  $x-y$  and  $x-z$  planes are close to the vertical line, which indicates that the initial momentum of  $\text{C}^+$  is much smaller than that of  $\text{F}^+$  and  $\text{Cl}^+$ .

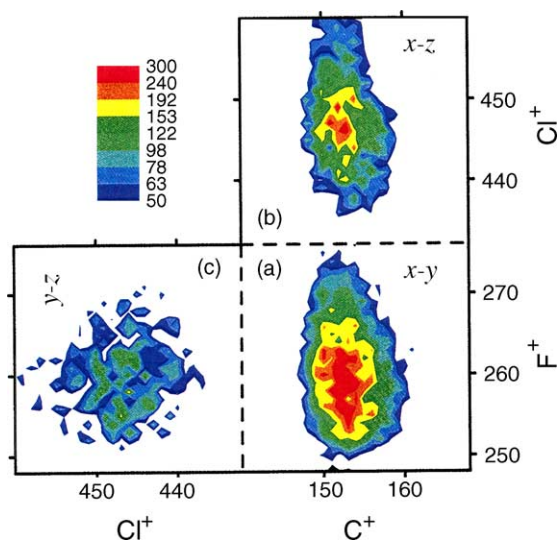


Fig. 4. The projections of the cell  $\text{COFCI}^{3+} \rightarrow \text{C}^+ + \text{F}^+ + \text{Cl}^+ + \text{O}$  on the (a)  $x-y$ , (b)  $x-z$ , and (c)  $y-z$  planes.

Because the island on the  $x-y$  plane is less tilted than that on the  $x-z$  plane, the momentum of  $\text{F}^+$  must be larger than that of  $\text{Cl}^+$ .

### 3.2. Cross sections for the different dissociation channels

The partial cross sections for electron impact dissociative ionization of  $\text{COFCI}$ , i.e.,  $\sigma(\text{X}^+)$  and  $\sigma(\text{X}^{2+})$ , are listed in column *a* of Table 2. We observed  $\text{COCl}^{2+}$  in the mass spectrum, since  $\text{CO}^{35}\text{Cl}^{2+}$  locates on the shoulder of  $\text{CF}^+$ , the cross section of  $\text{COCl}^{2+}$  is estimated from  $\text{CO}^{37}\text{Cl}^{2+}$ , using the isotopic abundance of  $^{35}\text{Cl} : ^{37}\text{Cl} = 1 : 0.32$ . The total cross section, by summing up  $\sigma(\text{X}^+)$  and  $\sigma(\text{X}^{2+})$ , is  $5.22 \times 10^{-16} \text{ cm}^2$ . The cross sections for the dissociation of  $\text{COFCI}$  monocations, i.e.,  $\sigma_1(\text{X}^+)$  for  $\text{COFCI}^+ \rightarrow \text{X}^+ + \text{n}$ , are listed in column *b* of Table 2. The total cross section of single ionization, by summing up  $\sigma_1(\text{X}^+)$ , is  $4.76 \times 10^{-16} \text{ cm}^2$ . Only 3.8% of the  $\text{COFCI}^+$  ions are stable and others undergo dissociation. The major ionic products are  $\text{COF}^+$  and  $\text{Cl}^+$ , they account for 44% of the dissociation of  $\text{COFCI}^+$ . This indicates that the breaking of C–Cl bond is the main pathway for the dissociation of  $\text{COFCI}^+$ .

The cross sections for the dissociation channels  $\text{COFCI}^{2+} \rightarrow \text{X}^{2+} + \text{n}$ , i.e.,  $\sigma_2(\text{X}^{2+})$  are also listed in column *b* of Table 2. The cross sections for  $\text{COFCI}^{2+} \rightarrow \text{X}^+ + \text{Y}^+ + \text{n}$ , i.e.,  $\sigma_2(\text{X}^+, \text{Y}^+)$  are listed in Table 3. The total cross section of double ionization, by summing up  $\sigma_2(\text{X}^{2+})$  and  $\sigma_2(\text{X}^+, \text{Y}^+)$ , is  $0.193 \times 10^{-16} \text{ cm}^2$ . All the  $\text{COFCI}$  dications are unstable and undergo dissociation. The ion-pair dissociation channels, i.e.,  $\text{COFCI}^{2+} \rightarrow \text{X}^+ + \text{Y}^+ + \text{n}$  are the main pathways, which account for 76% of the dissociation of  $\text{COFCI}^{2+}$ . The first few abundant dissociation channels are  $\text{COFCI}^{2+} \rightarrow \text{CO}^+ + \text{Cl}^+ + \text{F}$ ,  $\text{COFCI}^{2+} \rightarrow \text{C}^+ + \text{O}^+ + \text{n}$  and  $\text{COFCI}^{2+} \rightarrow \text{COF}^+ + \text{Cl}^+$ . The three highest occupied molecular orbitals of neutral  $\text{COFCI}$  are  $(15a')^2(4a'')^2(16a')^2$ , all of them are linear combinations

Table 2

The partial cross sections ( $10^{-19} \text{ cm}^2$ ) for electron impact dissociative ionization of  $\text{COFCI}$  (*a*), and the cross sections for the dissociation channels  $\text{COFCI}^+ \rightarrow \text{X}^+ + \text{n}$  and  $\text{COFCI}^{2+} \rightarrow \text{X}^{2+} + \text{n}$  (*b*)

	<i>a</i>	<i>b</i>
$\text{COFCI}^+$	181	181
$\text{COCl}^+$	173	171
$\text{COF}^+$	1080	1060
$\text{Cl}^+$	1150	1030
$\text{COCl}^{2+}$	14.0	14.0
$\text{CF}^+$	163	149
$\text{CO}^+$	539	504
$\text{COF}^{2+}$	6.03	5.72
$\text{F}^+$	544	486
$\text{Cl}^{2+}$	29.0	19.5
$\text{O}^+$	712	629
$\text{C}^+$	619	549
$\text{F}^{2+}$	1.45	1.09
$\text{O}^{2+}$	2.95	2.42
$\text{C}^{2+}$	3.34	2.67

The electron energy is 200 eV.



Table 3

The cross sections ( $10^{-19} \text{ cm}^2$ ) for the dissociation channels  $\text{COFCI}^{2+} \rightarrow \text{X}^+ + \text{Y}^+ + n$  and  $\text{COFCI}^{3+} \rightarrow \text{X}^{2+} + \text{Y}^+ + n$ 

	$\text{C}^{2+}$	$\text{O}^{2+}$	$\text{F}^{2+}$	$\text{C}^+$	$\text{O}^+$	$\text{Cl}^{2+}$	$\text{F}^+$	$\text{COF}^{2+}$	$\text{CO}^+$	$\text{CF}^+$	$\text{Cl}^+$
$\text{COCl}^+$							2.28				
$\text{COF}^+$						0.24					20.3
$\text{Cl}^+$	0.24	0.21	0.12	18.9	14.7		4.10	0.32	26.6	5.81	
$\text{CF}^+$					3.98	0.33					
$\text{CO}^+$						0.64	2.25				
$\text{F}^+$	0.16	0.19		10.4	15.4	2.16					
$\text{Cl}^{2+}$				2.23	3.88						
$\text{O}^+$	0.27		0.15	23.2							
$\text{C}^+$		0.13	0.09								

The electron energy is 200 eV.

Table 4

The cross sections ( $10^{-19} \text{ cm}^2$ ) for the dissociation channels  $\text{COFCI}^{3+} \rightarrow \text{X}^+ + \text{Y}^+ + \text{Z}^+ + n$ 

Dissociation channel	Cross section
$\text{C}^+ + \text{O}^+ + \text{F}^+ + \text{Cl}$	3.75
$\text{C}^+ + \text{O}^+ + \text{Cl}^+ + \text{F}$	6.61
$\text{C}^+ + \text{F}^+ + \text{Cl}^+ + \text{O}$	5.09
$\text{O}^+ + \text{F}^+ + \text{Cl}^+ + \text{C}$	7.19
$\text{O}^+ + \text{CF}^+ + \text{Cl}^+$	4.08
$\text{F}^+ + \text{CO}^+ + \text{Cl}^+$	5.18

The electron energy is 200 eV.

of Cl and O orbitals [9]. Removing electrons from these orbitals may weaken the C–Cl and C–O bond, thus the cleavages of these two bonds play significant roles in the dissociation of  $\text{COFCI}^+$  and  $\text{COFCI}^{2+}$ . Among the ion-pair dissociation channels of  $\text{COFCI}^{2+}$ , the cross section for different channels varies more than one order of magnitude.

All the triply ionized  $\text{COFCI}$  dissociate through  $\text{COFCI}^{3+} \rightarrow \text{X}^{2+} + \text{Y}^+ + n$  or  $\text{COFCI}^{3+} \rightarrow \text{X}^+ + \text{Y}^+ + \text{Z}^+ + n$ . Their cross sections, i.e.,  $\sigma_3(\text{X}^{2+}, \text{Y}^+)$  and  $\sigma_3(\text{X}^+, \text{Y}^+, \text{Z}^+)$  are listed in Tables 3 and 4, respectively. The total triple ionization, by summing up  $\sigma_3(\text{X}^{2+}, \text{Y}^+)$  and  $\sigma_3(\text{X}^+, \text{Y}^+, \text{Z}^+)$ , is  $0.043 \times 10^{-16} \text{ cm}^2$ . The ion-triple dissociation channels, i.e.,  $\text{COFCI}^{3+} \rightarrow \text{X}^+ + \text{Y}^+ + \text{Z}^+ + n$  are the major pathways, which contribute 74% to the dissociation of  $\text{COFCI}^{3+}$ . It is notable that for different ion-triple dissociation channels, the cross section varies not too much. The most abundant channel  $\text{O}^+ + \text{F}^+ + \text{Cl}^+ + \text{C}$  is less than two times of the weakest channel  $\text{C}^+ + \text{O}^+ + \text{F}^+ + \text{Cl}$ .

#### 4. Conclusions

We have probed the dissociation of singly to triply ionized carbonyl chlorofluoride ( $\text{COFCI}$ ) produced by electron impact ionization at an electron energy of 200 eV. Two- and three-dimensional covariance mapping techniques are used to identify the different dissociation channels. The absolute cross sections for the various dissociation channels of up to triply ionized  $\text{COFCI}$  have been obtained. By studying the orientation angles of the islands on the covariance map, the ion-pair dissociation channels of  $\text{COFCI}^{2+} \rightarrow \text{CO}^+ + \text{Cl}^+$

+ F and  $\text{COFCI}^{2+} \rightarrow \text{CF}^+ + \text{Cl}^+ + \text{O}$  are interpreted as sequential dissociations, where the first step is  $\text{COFCI}^{2+} \rightarrow \text{COF}^+ + \text{Cl}^+$ , and the second step  $\text{COF}^+ \rightarrow \text{CO}^+ + \text{F}$  or  $\text{COF}^+ \rightarrow \text{CF}^+ + \text{O}$  occurs within the effective Coulomb field of the  $\text{Cl}^+$  ion. The  $\text{COFCI}$  dications dissociate mainly into ion pairs with a variety of cross sections, and the major dissociation channels are  $\text{CO}^+ + \text{Cl}^+ + \text{F}$ ,  $\text{C}^+ + \text{O}^+ + n$  and  $\text{COF}^+ + \text{Cl}^+$ . The  $\text{COFCI}$  trications dissociate mainly into ion triples, with a comparable cross section for each dissociation channel.

#### Acknowledgements

A major part of this work was performed in the Max Planck Institute for Quantum Optics. We thank Dr Werner Fuss, Dr Hartmut Schroeder, and Dr Jochen Wanner for their valuable assistances. The technical help of Bernd Steffes is appreciated. P. Wang is grateful to the Alexander von Humboldt Foundation for providing the financial support for staying at the Max Planck Institute for Extraterrestrial Physics.

#### References

- [1] W.M. Huo, Y.-K. Kim, IEEE Trans. Plasma. Sci. 27 (1999) 1225.
- [2] E. Meeks, P. Ho, Thin Solid Films 365 (2000) 334.
- [3] E. Herbst, C.M. Leung, Astrophys. J. Suppl. Ser. 69 (1989) 271.
- [4] D. Mathur, Phys. Rep. 225 (1993) 193.
- [5] D. Schröder, H. Schwarz, J. Phys. Chem. A 103 (1999) 7385.
- [6] R.K.M. Jayanty, R. Simonaitis, J. Heicklen, J. Photochem. 4 (1974) 381.
- [7] A. Noelle, C. Krumscheid, H. Heydtmann, Chem. Phys. Lett. 299 (1999) 561.
- [8] C. Maul, C. Dietrich, T. Haas, K.-H. Gericke, Phys. Chem. Chem. Phys. 1 (1999) 1441.
- [9] P. Sherwood, E.A. Seddon, M.F. Guest, M.J. Parkington, T.A. Ryan, K.R. Seddon, J. Chem. Soc. Dalton Trans. (1995) 2359.
- [10] K. Hinds, J.H. Holloway, A.C. Legon, Chem. Phys. Lett. 242 (1995) 407.
- [11] A. Perrin, J.-M. Flaud, H. Buerger, G. Pawelke, S. Sander, H. Willner, J. Mol. Spectrosc. 209 (2001) 122.
- [12] N. Heineking, W. Jaeger, M.C.L. Gerry, J. Mol. Spectrosc. 158 (1993) 69.

- [13] J. Demaison, A. Perrin, H. Buerger, *J. Mol. Spectrosc.* 221 (2003) 47.
- [14] M. Hermann, A. Noelle, H. Heydtmann, *Chem. Phys. Lett.* 226 (1994) 559.
- [15] J.S. Francisco, Z. Li, *J. Phys. Chem.* 93 (1989) 8118.
- [16] C. Maul, K.-H. Gericke, *J. Phys. Chem. A* 104 (2000) 2531.
- [17] C. Tian, C.R. Vidal, *Phys. Rev. A* 59 (1999) 1955.
- [18] C. Tian, C.R. Vidal, *Phys. Rev. A* 58 (1998) 3783.
- [19] C. Tian, C.R. Vidal, *J. Phys. B* 31 (1998) 5369.
- [20] C. Tian, C.R. Vidal, *J. Chem. Phys.* 108 (1998) 927.
- [21] L.J. Frasinski, K. Codling, P.A. Hatherly, *Science* 246 (1989) 1029.
- [22] H.C. Straub, P. Renault, B.G. Lindsay, K.A. Smith, R.F. Stebbings, *Phys. Rev. A* 52 (1995) 1115.
- [23] C. Ma, M.R. Bruce, R.A. Bonham, *Phys. Rev. A* 44 (1991) 2921.
- [24] B. Brehm, J. Grosser, T. Ruschinski, M. Zimmer, *Meas. Sci. Technol.* 6 (1995) 953.
- [25] M.R. Bruce, L. Li, C.R. Sporleder, R.A. Bonham, *J. Phys. B* 27 (1994) 5773.
- [26] J.H.D. Eland, *Mol. Phys.* 61 (1987) 725.
- [27] L.J. Frasinski, M. Stankiewicz, K.J. Randall, P.A. Hartherly, K. Codling, *J. Phys. B* 19 (1986) L819.
- [28] R. Thissen, J. Delwiche, J.M. Robbe, D. Duflo, J.P. Flament, J.H.D. Eland, *J. Chem. Phys.* 99 (1993) 6590.